

# A GENERALIZED STUDY OF PRECIPITATION FORECASTING

## PART 2: A GRAPHICAL COMPUTATION OF PRECIPITATION

P. M. KUHN

Short Range Forecast Development Section, U. S. Weather Bureau, Washington, D. C.

[Manuscript received August 27, 1953; revised September 23, 1953]

### ABSTRACT

A graphical technique for estimating areal precipitation patterns associated with given contemporary charts of streamlines and isotachs and of moisture at four selected levels is developed from the basic physical considerations presented by Thompson and Collins [1]. Procedures are described for calculating the vertical velocity at four selected levels by a kinematic method. The vertical velocities obtained are combined with a graphical solution of Fulks' formula for the rate of precipitation from pseudo-adiabatically ascending air and a method is derived for calculating the 12-hour rate of precipitation. An areal comparison is made of computed and observed precipitation.

### INTRODUCTION

As part of continuing research instituted by Thompson and Collins [1] for the general purpose of studying precipitation forecasting, attempts are being made to extend and to modify their technique in such a way as to enable the areal distribution of precipitation to be computed graphically. This paper is a description of the development and testing of one solution to the problem.

Proceeding on a purely physical basis, Thompson and Collins employed in their pilot study observed winds to compute divergence over a triangular area in the Midwest. From this divergence vertical motion was then derived using continuity considerations and, with observed moisture, was used to compute the average rate of precipitation over the area. Their procedure was completely numerical and designed for either hand or machine computation, requiring only the wind and RAOB data obtained from soundings at the vertices of the triangle. Effects of subjective analysis of the data were thus purposely eliminated.

On the other hand, in the present investigation, computations were made using carefully analyzed standard-level maps, combining the parameters derived from the wind and moisture fields by graphical addition, subtraction, and multiplication. Since one of the purposes of this study was the further testing of the usefulness of observed winds in estimating precipitation over large area, the physical model used by Thompson and Collins was retained with only a few necessary changes in the computational constants.

### THE BASIC PHYSICAL MODEL

In the basic model it was assumed that the rate of precipitation depended only on the vertical motion of the

air column and the moisture contained therein. Non-adiabatic effects of radiation, evaporation, and cloud storage were neglected, as were orographic and frictional influences on the vertical motion. An expression derived by Fulks [2] was used to compute the rate of precipitation. The rate of precipitation,  $r$ , from a shallow layer of saturated air ascending pseudo-adiabatically is given by:

$$r = \left[ \frac{\epsilon}{RT} \left( \frac{de}{dz} + \frac{eg}{RT} \right) \right] V_z \Delta z = I V_z \Delta z \quad (1)$$

where

$\epsilon$  is the ratio of the density of water vapor to that of dry air at constant pressure and temperature

$R$  is the gas constant for dry air

$T$  is the mean absolute temperature of the layer

$e$  is the saturation vapor pressure of the layer

$z$  is the height

$g$  is the acceleration due to gravity

$V_z$  is the vertical velocity in the layer, positive upward

$\Delta z$  is the thickness of the layer

Fulks' expression assumes that the air is saturated throughout the period in which it is being lifted. In order to take into account the frequent case in which the atmosphere is not initially saturated, Thompson and Collins defined an "effective" vertical velocity which would produce the same amount of precipitation in a given time if the air were initially saturated as would the actual vertical velocity with the air initially not saturated. This effective vertical velocity is given by:

$$V'_z = V_z + \frac{T_0 - T_{\infty}}{\Delta t \left( \frac{dT}{dz} - \frac{dT_d}{dz} \right)} \quad (2)$$

where  $V_z$  is the mean vertical velocity of the layer,  $T_0$  and  $T_{\infty}$  are the temperature and dew point within the layer,

respectively, with the subscript "0" denoting the value at the beginning of the time interval  $\Delta t$ . Making approximations for the lapse rates and performing the computations for a 12-hour period, the effective vertical velocity is given by:

$$V'_z = V_z - 0.28(T_0 - T_{a0}) \quad (3)$$

where vertical velocities are expressed in centimeters per second and temperatures in degrees Celsius.

The actual vertical velocity can be obtained by numerical integration of the equation of continuity, assuming that density varies only in the vertical and that the vertical velocity at the surface is zero. Then the vertical velocity,  $V_{z2}$ , at the top of a layer is given by:

$$V_{z2} = -\frac{1}{2} \left[ \frac{\rho_1}{\rho_2} D_1 + D_2 \right] \Delta z + \frac{\rho_1}{\rho_2} V_{z1} \quad (4)$$

where  $D$  is the horizontal velocity divergence,  $\rho$  is the density, and the subscripts 1 and 2 refer to the bottom and top of the layer, respectively.

The horizontal divergence is computed by a graphical method which will be described in a later section. Then from equations (1) through (4) the contribution,  $r_i$ , by each of several layers is computed. The total rate of precipitation,  $P$ , over the area is then found by summing over the layers.

$$P = \sum_i r_i$$

where the index  $i$  ranges over all layers from the surface to the top of the atmosphere. In practice, the summation can usually be terminated at 500 mb. since the layers above have too little moisture to contribute significant amounts.

#### ADAPTATION OF BASIC MODEL FOR GRAPHICAL ANALYSIS

In the present study, two major modifications of the basic model were made. Instead of computing precipitation for a single triangle, computations were made for a net of triangles covering the eastern half of the United States (east of  $100^\circ$  W.), and a streamline-isotach analysis was used to provide wind data instead of relying on the winds reported at certain sounding stations. Since preliminary tests indicated that computations for only four levels, 950, 850, 700 and 500 mb. gave essentially the same precipitation values as computations for a stratification into more layers, only these four were used.

Horizontal velocity divergence was obtained by an extension of the method suggested by Bennett [3] and Bellamy [4]. Instead of using observed winds at only those vertices coinciding with winds-aloft stations, a streamline-isotach analysis was made. This permitted a grid, consisting of many adjacent equilateral triangles to be used. A transparent overlay, hereafter called Divergence Grid, was designed for a map with scale factor of

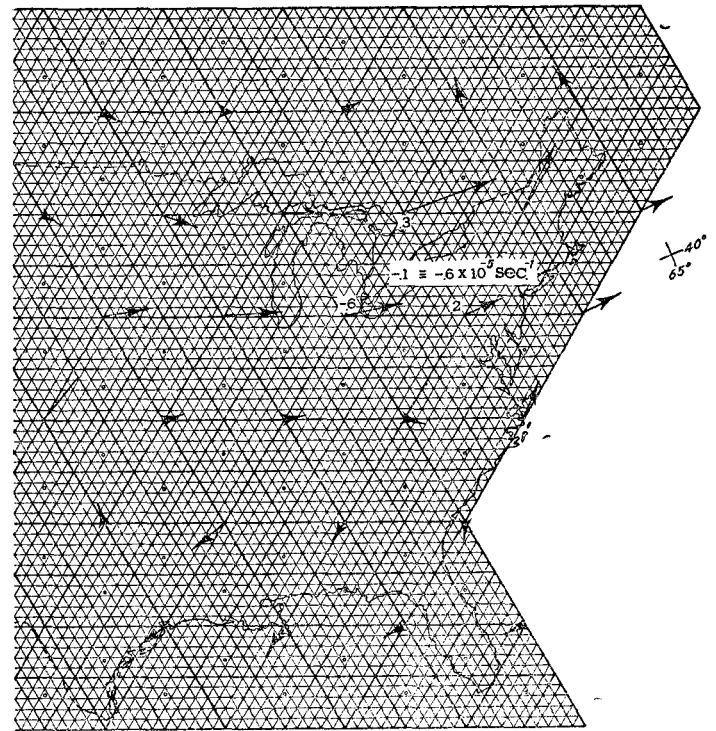


FIGURE 1.—Portion of divergence grid used in computing horizontal velocity divergence. Vectors at 950 mb. for 0300 GMT, December 28, 1949, have been constructed at the vertices of each equilateral triangle in the grid. Numbers show the values of the partial divergence in units per 5 hours, for one triangle. Their sum is the total divergence, converted here to units per second and plotted at the center of the triangle.

1:12,500,000. This Divergence Grid, containing 109 triangles, is reproduced on smaller scale in figure 1. It was not considered necessary to modify the grid to correct for divergence of the meridians or for slight map distortion.

Several advantages can be claimed for the use of a streamline-isotach analysis. In the first place, calculations are not dependent on data from a given station, and no days or areas need be lost because of missing soundings. Further, the smoothing involved in the analysis may tend to eliminate errors and winds of a scale so small as not to be commensurate with the grid size. This procedure differs from that of Graham [5] in that a large grid of symmetrical triangles is employed rather than a single, movable triangle. Also streamlines are drawn instead of isogons.

Since all the grid triangles are identical, a series of thin lines, parallel to the sides of the triangles, can be constructed so that each of the three equal altitudes of every triangle is divided into ten equal intervals. These divisions, in the form of parallel lines, facilitate the computation of the partial divergences. With their aid the partial divergences can easily and quickly be read to increments of 5 percent.

The choice of 280 nautical miles as the optimum dimension for the sides of the triangles was based on the mean distance between adjacent reporting RAOB-RAWIN stations in the United States, about 230 miles, and the size of the smallest disturbance which it was felt could be treated by large-scale methods, about 300 miles.

If values for the density variation in the vertical and for the distance between pressure surfaces is approximated by U. S. Standard Atmosphere values, equation (4) can be evaluated for each of the four levels, 950, 850, 700 and 500 mb. These simplified equations are:

$$V_{z950} = -0.44 D_{950} \tag{5}$$

$$V_{z850} = 1.09 V_{z950} - 0.50 D_{950} - 0.46 D_{850} \tag{6}$$

$$V_{z700} = 1.17 V_{z850} - 0.91 D_{850} - 0.77 D_{700} \tag{7}$$

$$V_{z500} = 1.31 V_{z700} - 1.68 D_{700} - 1.28 D_{500} \tag{8}$$

Equations (5) and (6) were further simplified by assuming that  $-0.44 D_{950}$  is approximately equal to  $-0.50 D_{950}$ , that  $(1.09 V_{z950} - 0.50 D_{950})$  is approximately equal to  $-D_{950}$ , and that  $-0.46 D_{850}$  is approximately equal to  $-0.50 D_{850}$ . Equations (5) and (6) then become:

$$V_{z950} = -0.50 D_{950} \tag{5a}$$

$$V_{z850} = -D_{950} - 0.50 D_{850} \tag{6a}$$

Using these equations, the vertical velocity at each of the four levels can be computed by graphical means.

Similarly equation (1) can be modified and condensed for graphical computation. If the modification for non-saturation is made, the contribution of a given layer to the total rate of precipitation is

$$r = V'_z I k \tag{9}$$

where  $r$  is the rate in inches per 12 hours contributed by the layer,  $V'_z$  is the effective vertical velocity in centimeters per second,  $I$ , the expression in the brackets in equation (1), is determined from a diagram developed by Fulks [2], and  $k$  is a factor (constant for a given level) which includes the Standard Atmosphere thickness and conversion constants for changing units. For convenience in computation, table 1 of values of  $I k$  was prepared for the various temperatures encountered at the four levels. Thus to obtain the contribution of a given level, we simply multiply graphically  $V'_z$  by  $I k$ . Total precipitation,  $P$ , for the 12-hour period is then given by

$$P = r_{950} + r_{850} + r_{700} + r_{500} \tag{10}$$

where again the addition is carried out graphically.

GRAPHICAL PROCEDURES

The preceding description of the basic physical model and its adaptation for graphical analysis indicates a requirement for three basic sets of isopleth fields in the computation of a quantitative precipitation pattern: (1) the field of divergence of horizontal velocity at the 950-, 850-, 700- and 500-mb. levels; (2) the field of vertical velocity (isanabats) at these levels; and (3) the field of moisture,

TABLE 1—Tabular values of the factor  $I k$  for given temperatures and selected pressure surfaces

Temp. °C	950 mb.	850 mb.	700 mb.	500 mb.
20	.04	.05	.06	.08
19				
18				
17				
16				
15	.04			.08
14	.03			.07
13				
12				
11				
10			.06	
9		.05	.05	
8		.04		
7				
6				
5				.07
4				.06
3				
2				
+1	.03		.05	
0	.02		.04	
-1		.04		.06
-2		.03		.05
-3				
-4				
-5				
-6			.04	
-7			.03	
-8				.05
-9		.03		.04
-10		.02		
-11				
-12	.02			.04
-13	.01		.03	.03
-14			.02	
-15				
-16				
-17		.02		
-18		.01		
-19				
-20				
-21			.02	.03
-22			.01	.02
-23				
-24				
-25	.01			
-26				
-27				
-28				
-29				
-30		.01	.01	.02

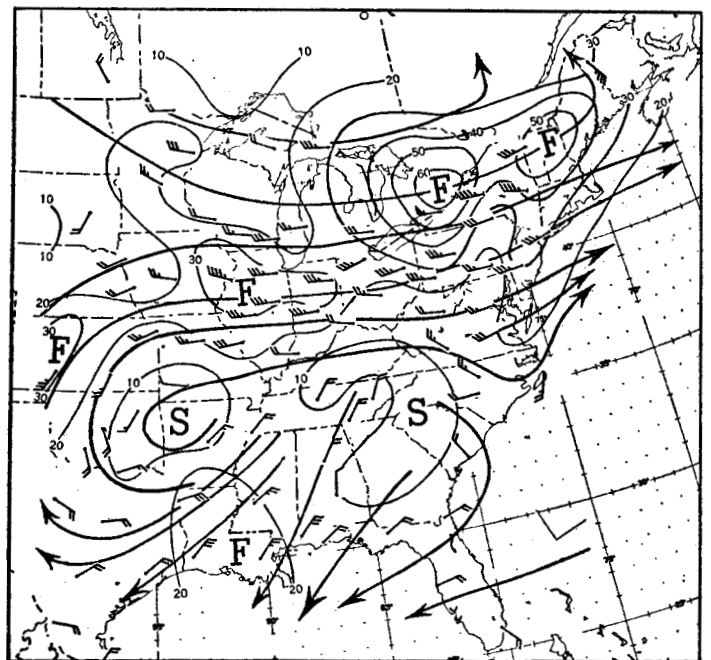


FIGURE 2.—Streamline-isotach field at 950 mb. for 0300 GMT, December 28, 1949. Arrowed lines are streamlines everywhere tangent to the observed winds (full barb equals 10 knots). Thin solid lines are isotachs in increments of 10 knots.

expressed by isopleths of 0.28 ( $T_0 - T_{a0}$ ), at these levels. These three fields are all obtained and combined graphically to provide the final isohyetal field. The Appendix contains a detailed description of the individual operations that will enable others to perform the computations, but the following brief summary is provided for the reader interested in only the broad outline of the procedures.

Initially, the divergence is computed, with the aid of the Divergence Grid (fig. 1), from a streamline-isotach analysis (fig. 2) for each level. The resulting fields of divergence are graphically combined in accordance with equations (5a), (6a), (7), and (8) to obtain the fields of vertical velocity (figs. 3-6). Graphical subtraction of the moisture field (fig. 7) from the vertical velocity field,

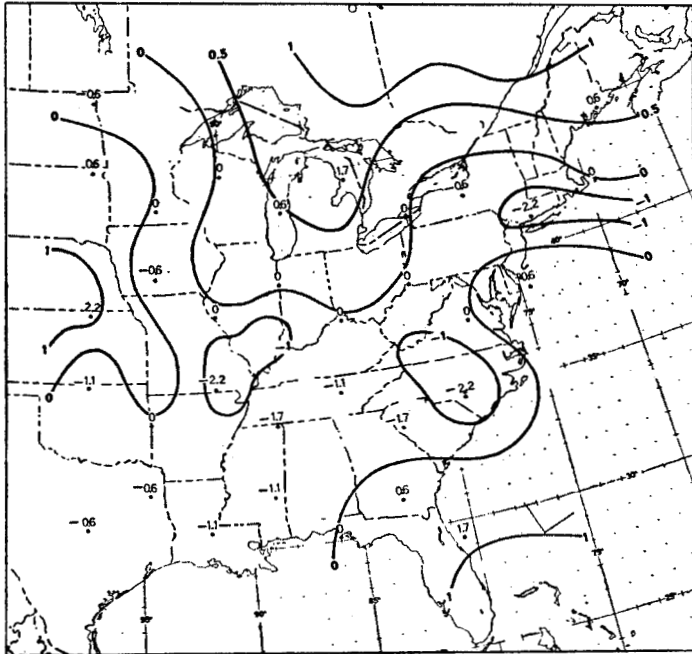


FIGURE 3.—Isanabats in  $\text{cm. sec}^{-1}$  at 950 mb., 0300 GMT, December 28, 1949. Positive values indicate ascent and negative values descent. Plotted values are divergences in units of  $10^{-3} \text{ sec}^{-1}$  computed from the field of figure 2 by use of the grid of figure 1. Positive signs indicate convergence and negative, divergence. The 950-mb. vertical velocity is equal to  $-0.50D_{950}$  from equation (5a).

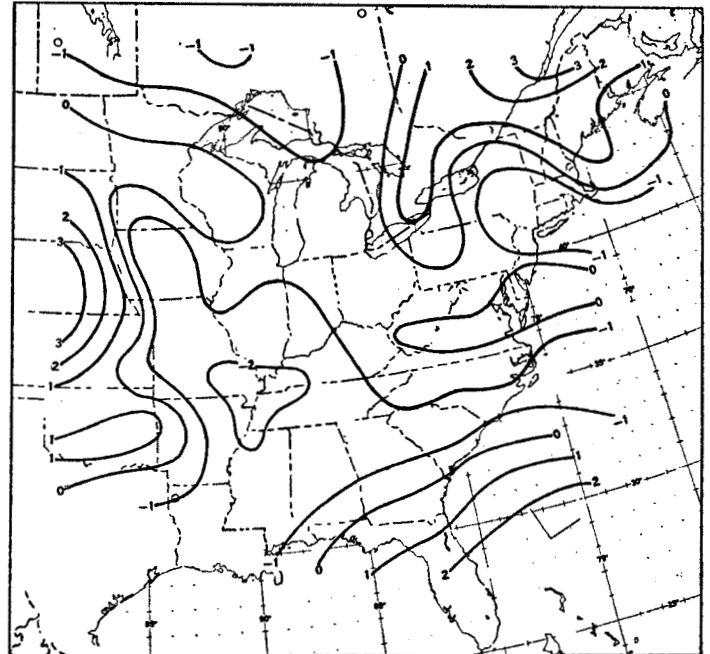


FIGURE 5.—Isanabats in  $\text{cm. sec}^{-1}$  at 850 mb. for 0300 GMT, December 28, 1949 (dashed lines of fig. 4). Positive values indicate ascent and negative, descent. This chart represents the graphical solution of equation (6a).

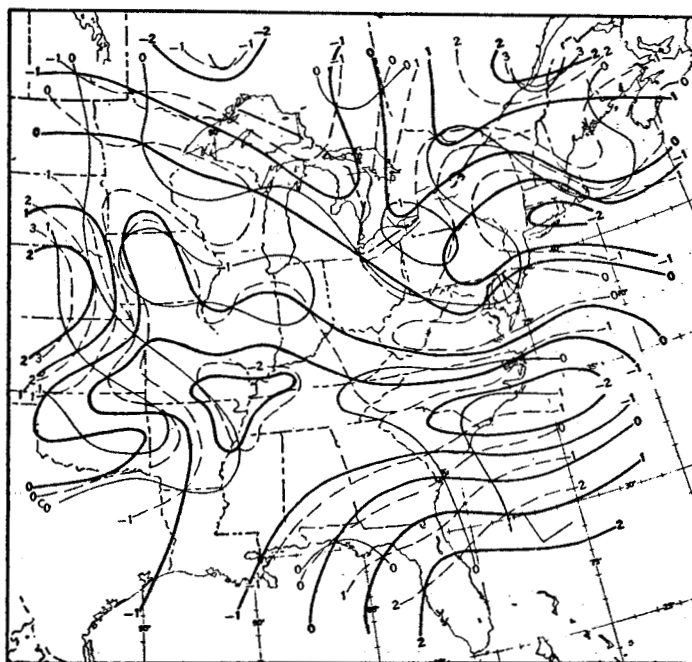


FIGURE 4.—Graphical summation following equation (6a) of  $-D_{850}$  (heavy solid lines) and  $-0.50D_{950}$  (thin solid lines) to produce the isanabats in  $\text{cm. sec}^{-1}$  at 850 mb. (dashed lines) for 0300 GMT, December 28, 1949. Positive values indicate ascent and negative, descent. The vertical velocity analysis is shown separately in figure 5.

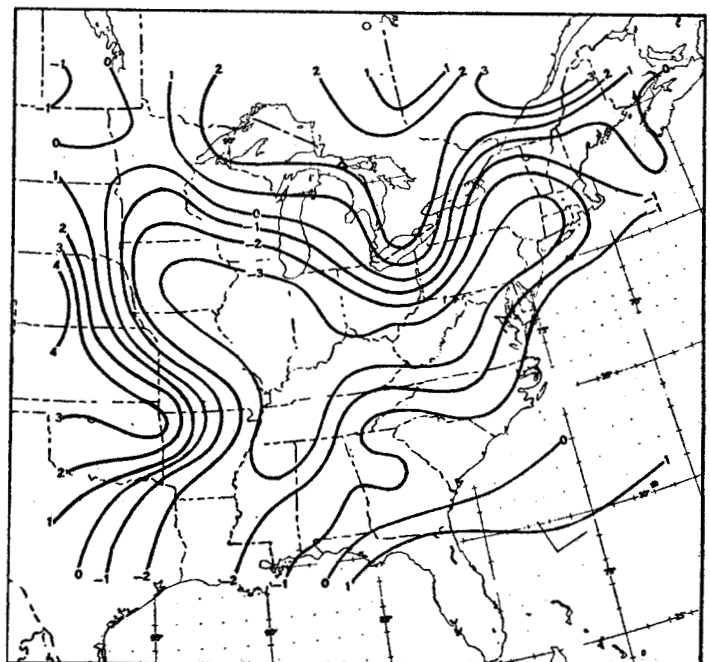


FIGURE 6.—Isanabats in  $\text{cm. sec}^{-1}$  at 700 mb. for 0300 GMT, December 28, 1949. This field represents the graphical solution of equation (7). Positive values indicate ascent and negative, descent.

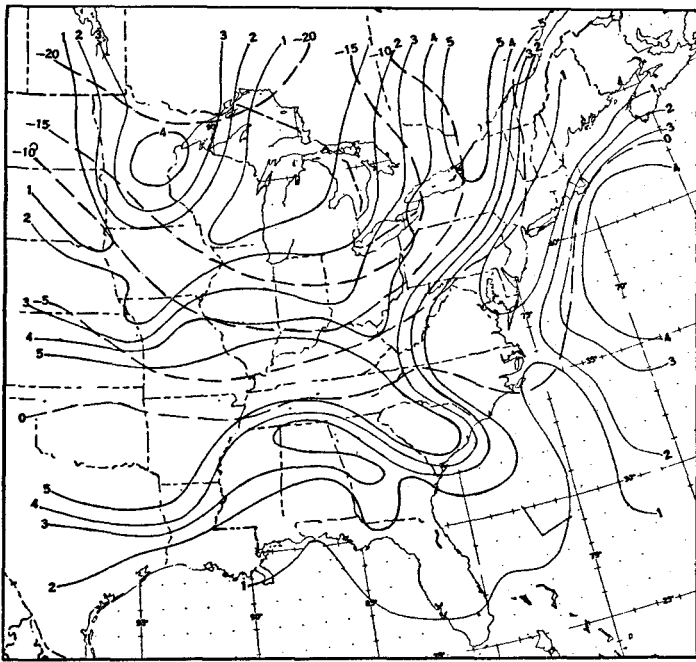


FIGURE 7.—Solid lines show isopleths of  $0.28 (T_0 - T_{d0})$ , the moisture term defined in equations (2) and (3), for the 700-mb. level, 0300 GMT, December 28, 1949. Isotherms in ° C. at 700 mb. required in the evaluation of the  $Ik$  term (equation (9)) at this level are shown by dashed lines. See figure 8 for next step in obtaining the effective vertical velocity,  $V'_e$ .

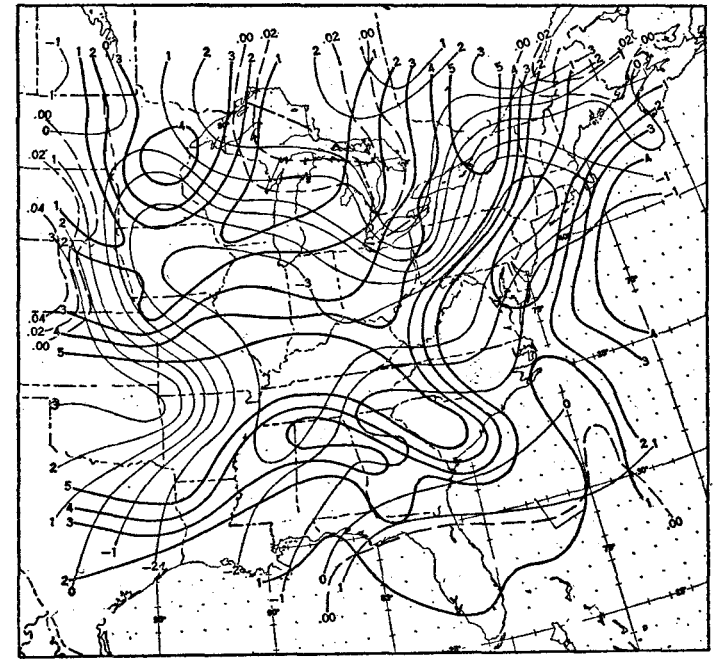


FIGURE 8.—Isohyets (thin dashed lines) computed for 700-mb. level, 0300 GMT, December 28, 1949, by graphical subtraction of  $0.28 (T_0 - T_{d0})$  field (heavy solid lines) from isanabatic field (thin solid lines). The isolines of  $V'_e$  resulting from this subtraction (equation (3)) have here been converted by multiplication by the  $Ik$  factor (equation (9) and table 1), to precipitation in inches.

in accordance with equation (3), gives the field of effective vertical velocity, (fig. 8). The isolines of effective vertical velocity, when multiplied by  $Ik$  (see equation (9)), represent isohyets for each layer (fig. 8). Finally, graphical summation of the isohyets for the 950-, 850-, 700-, and 500-mb. levels gives the total isohyetal pattern in accordance with equation (10).

The extensive use of graphical addition and subtraction, rather than successive grid additions, which require the reading of data from grid points and performing calculations for each such point, greatly reduced the computational time. Moreover, as Fjrtoft [6] has pointed out, the analyzed map is used nearly everywhere in graphical analysis, whereas in grid analysis the points of the grid may often be in unfavorable positions for sufficiently accurate evaluation. Graphical analysis also gives the isopleth field directly, requiring no further analysis.

### TEST COMPUTATIONS

Computed precipitation charts for 12-hour periods were analyzed and verified for 14 experimental cases from the 25th through the 31st of December, 1949. This particular period was chosen since it provided two complete cycles from dry to wet weather regimes over the eastern half of the United States.

The extent of the coincidence of the computed and observed "rain-no rain" patterns is most clearly illustrated by superimposing these patterns on the same base chart (figure 10). A measure of the degree of agreement for all cases studied was obtained by use of contingency

tables, percentage correct, and skill score. Sixty-eight first-order stations east of the 100th meridian were selected to sample the area, and observations from these stations were used in this part of the verification.

To examine the quantitative precipitation computations, observed precipitation maps were plotted from the hourly precipitation data for all recording gages as reported in *Climatological Data for the United States by Sections*, U. S. Department of Commerce, Weather Bureau, December 1949. The observed isohyetal field was analyzed and a quantitative comparison with the computed field was made for a number of periods.

### INDIVIDUAL EXAMPLES

Of particular interest were the computations for the three 12-hour periods between 1500 GMT on the 25th and 0300 GMT on the 27th of December 1949, since the results for this interval indicated the effectiveness with which this technique computed the precipitation associated both with a cold front advancing through the Midwest and a warm front moving northward up the Florida Peninsula.

Each of the three 12-hour periods is illustrated (figs. 9–12) with a surface chart, corresponding 700-mb. chart, and the computed and observed precipitation charts. Before discussing the examples, it may be well to mention that for these 3 cases the isanabatic field employed in computing the effective vertical velocity,  $V'_e$  was the mean of the fields derived for the beginning and the end of the 12-hour interval.

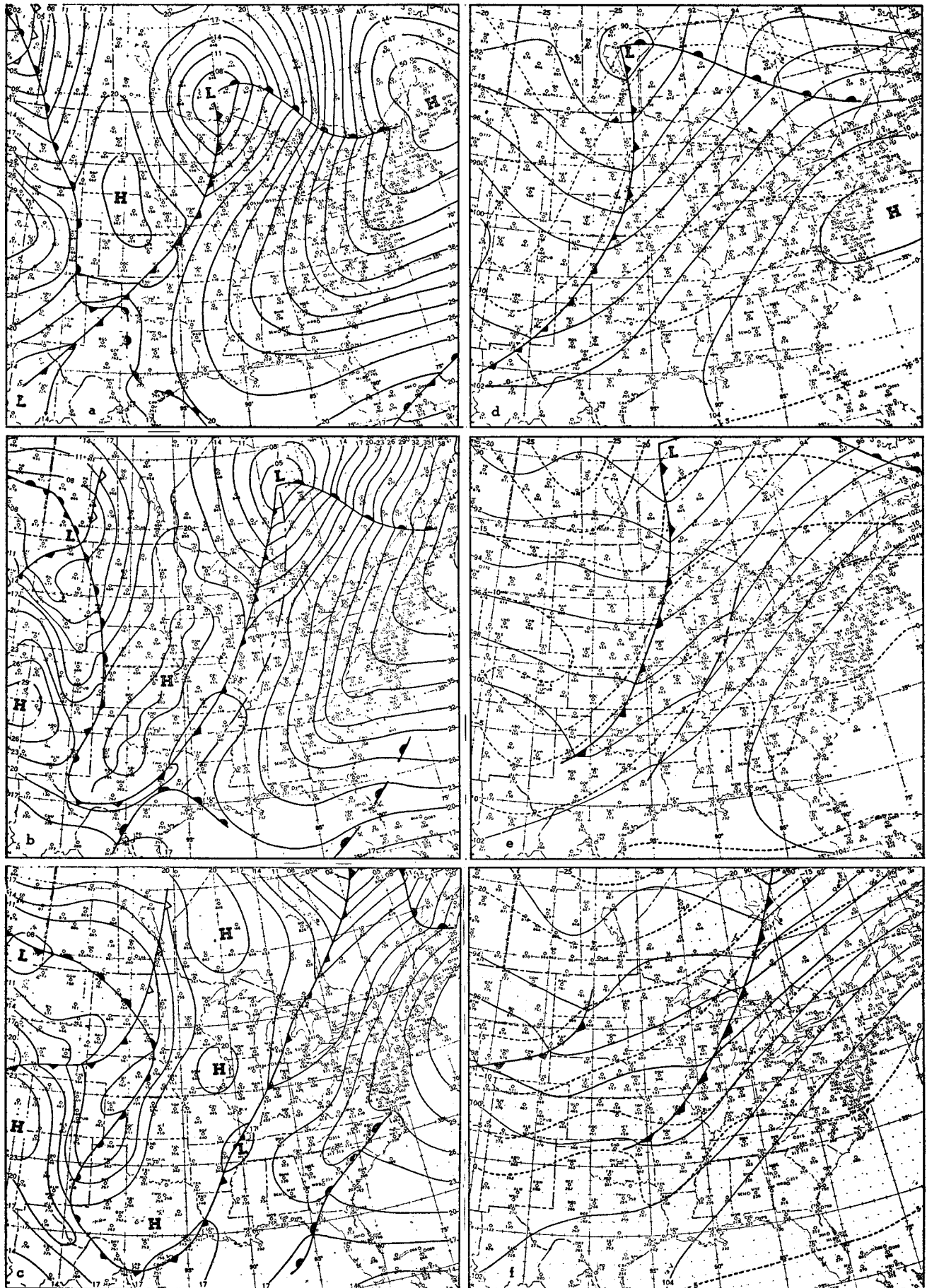


FIGURE 9.—Series of charts illustrating the surface and 700-mb. conditions at the times of the three examples of computed and observed precipitation shown in figures 10-14. Parts a, b, and c are surface charts for 1830 GMT, December 25, 1949; 0630 GMT, December 26, 1949; and 1830 GMT, December 26, 1949, respectively. Parts d, e, and f are the 700-mb. charts for the 1500 GMT and 0300 GMT observation times, corresponding to the surface charts, in the same order.

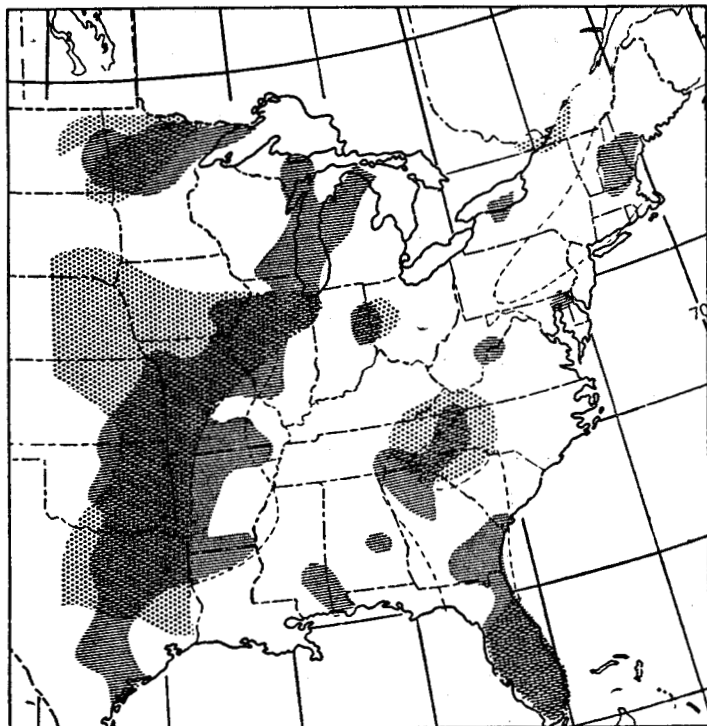


FIGURE 10.—Computed and observed precipitation patterns for 12-hour period 1500 GMT, December 25 to 0300 GMT, December 26, 1949. Observed precipitation areas are shown by cross hatching, computed areas by stippling. Amount of overlapping is an indication of accuracy of method. Thin dashed lines enclose areas for which precipitation was indicated by the computations for the 700-500-mb. layer only.

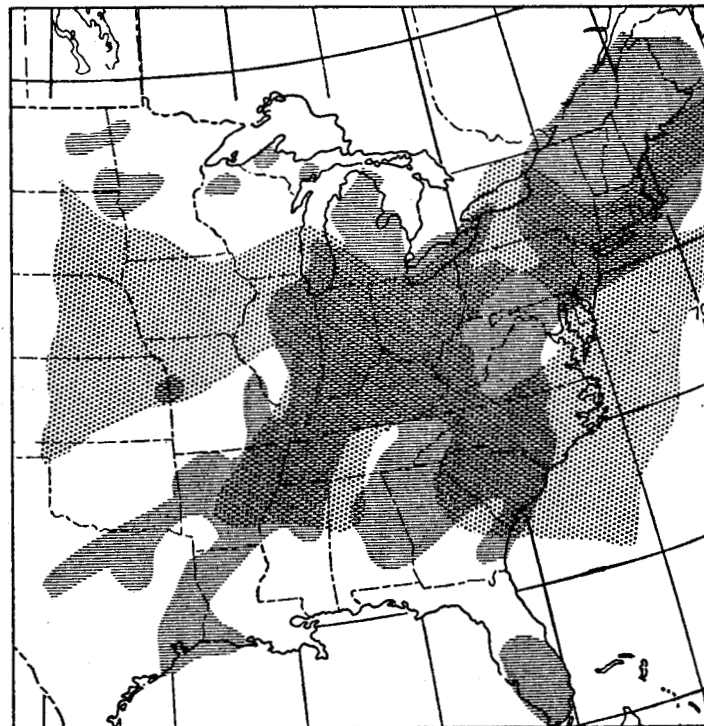


FIGURE 12.—Computed and observed precipitation patterns for the 12-hour period 0300 GMT, December 26 to 0300 GMT December 27, 1949. Observed precipitation areas are shown by cross hatching, computed areas by stippling.

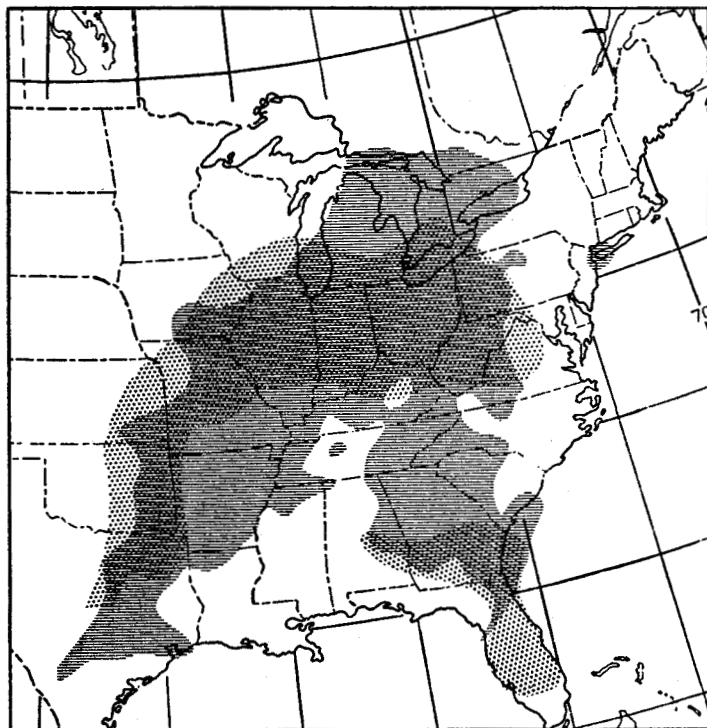


FIGURE 11.—Computed and observed precipitation patterns for the 12-hour period 0300 to 1500 GMT, December 26, 1949. Observed precipitation areas are shown by cross hatching, computed areas by stippling.

1500 GMT December 25-0300 GMT December 26, 1949.—  
The generally satisfactory verification (fig. 10) for

Florida, eastern Tennessee, and western North Carolina, seemed particularly significant in that it indicated the ability of the analytic computation to compute most of the area in which precipitation occurred in advance of the warm front that crossed southern Florida during the period. The spotty rain areas along the east coastal area apparently were due to local convective features of a smaller scale than this technique attempts to measure, and to orographic effects which have been neglected. The area for which precipitation was indicated only by the 500-mb. vertical motion pattern and not by lower levels is inclosed by the dashed line in figure 10. Since little precipitation was observed within this area, it is suspected that evaporation is an important factor which leads to such over-forecasting. However, high cloudiness did occur over these areas.

0300 GMT December 26-1500 GMT December 27, 1949.—  
The slowly moving cold front on a line from Houston, Tex. to Alpena, Mich. at the end of the period, and the incipient wave in the vicinity of Memphis, Tenn., together with the advancing warm front in the Southeast, brought copious rain areas to the eastern part of the United States. During this period, with well-defined large-scale systems and associated relatively broad fields of vertical motion, the computations fitted the observations well in most areas (fig. 11). Results were not satisfactory in the Southeast, but it is felt that neglect of orographic effects and the occurrence of convective instability on a local scale were responsible for the under-forecasting noted.

1500 GMT December 26-0300 GMT December 27, 1949.— This example seems to demonstrate the effect of neglecting downslope motion with its attendant "drying out" in the western zone of the computation area. For it is here that the computations show their most serious defect in over-forecasting (fig. 12). In this region the downslope motion due to the slope of the ground surface appeared to be effectively cancelling the upward motion indicated by the horizontal divergence pattern. The inclusion of an orographic correction term for the vertical motion and an evaporation correction term for higher level precipitation contributions should reduce the tendency to over-forecasting in certain regions.

VERIFICATION

In evaluating the significance of the results of computations demonstrated in the preceding examples, composite contingency tables were prepared. Verification was obtained by using a representative grid of 68 stations, as previously stated. Table 2 summarizes the results for five 12-hour periods for which mean isanabatic fields were used in the computations. The 3 test cases just illustrated were included in this period which ran from 0300 GMT, December 25, to 1500 GMT, December 27, 1949. Table 3 presents the same 5 cases when computations were made with the isanabatic field assumed to persist from the beginning of the 12-hour period throughout. It seems evident that the use of mean vertical velocities improves the results.

In all, 14 cases were computed on the assumption that the isanabatic field at the beginning of a 12-hour period persisted, covering the period 0300 GMT, December 25, 1949, to 0300 GMT, January 1, 1950. Table 4 is the contingency table for these 14 cases and summarizes the overall results for computations made in this manner.

Figures 13 and 14 exhibit the computed and observed isohyetal pattern for the period 1500 GMT, December 25, through 0300 GMT, December 26, 1949. In general, the results were not as satisfactory as the areal "rain-no rain" verifications. In this, as in four other cases studied, there was a general tendency for the heaviest computed rainfall to be somewhat less than the corresponding heaviest observed rainfall. (See table 5.) Also evident was some displacement of the centers of intensity.

TABLE 2.—Contingency table comparing computed and observed occurrence of precipitation for five 12-hour periods from 0300 GMT, December 25 through 0300 GMT, December 27, 1949. Computations of precipitation occurrence were based on isanabatic fields obtained by averaging the isanabatic fields at the beginning and end of each 12-hour period

		Computed			Skill score..... .44 Percent..... .74
		Rain	No rain	Total	
Observed	Rain.....	98	37	135	
	No rain.....	52	153	205	
	Total.....	150	190	340	

TABLE 3.—Contingency table comparing computed and observed occurrence of precipitation for five 12-hour periods from 0300 GMT, December 25 through 0300 GMT, December 27, 1949 (same 5 periods as in table 2). Computations of precipitation occurrence were based on assumption that isanabatic field at beginning of each period persists throughout the 12 hours

		Computed			Skill score..... .40 Percent..... .71
		Rain	No rain	Total	
Observed	Rain.....	95	40	135	
	No rain.....	60	145	205	
	Total.....	155	185	340	

TABLE 4.—Contingency table comparing computed and observed occurrence of precipitation for fourteen 12-hour periods from 0300 GMT, December 25 through 0300 GMT, December 31, 1949. Computations of precipitation occurrence based on assumption that isanabatic field at beginning of each period persists throughout the 12 hours.

		Computed			Skill score..... .40 Percent..... .72
		Rain	No rain	Total	
Observed	Rain.....	266	112	378	
	No rain.....	157	417	574	
	Total.....	423	529	952	

TABLE 5.—Contingency table for quantitative precipitation estimates and observations (in.) for five 12-hour periods from 0300 GMT, December 25 through 0300 GMT, December 27, 1949

		Computed					Total	Skill score..... .24 Percent..... .53
		0	.01-.10	.11-.20	.21-.50	>.50		
Observed	0	153	41	6	5	0	205	
	.01-.10	17	15	5	0	0	37	
	.11-.20	15	34	5	1	0	55	
	.21-.50	5	3	25	2	3	38	
	>.50	0	0	0	0	5	5	
	Total.....	190	93	41	8	8	340	

CONCLUSIONS

A graphical technique for estimating areal precipitation patterns associated with given flow patterns at standard levels has been derived from basic physical considerations. In a test of the model it was found that approximately 75 percent of the area was correctly estimated on a "rain-no rain" basis. This technique is not presented for use in current forecasting, since prognostic charts of streamlines and isotachs are not available for test purposes. However, some tentative conclusions can be drawn as to factors which must be included in any such generalized forecasting technique, and some hint is available as to their relative importance.

In all cases computed, the greatest precipitation contribution occurred in the layers between 950 mb. and 700 mb., although vertical velocities were greater in the higher layers. This points out that the moisture content is as

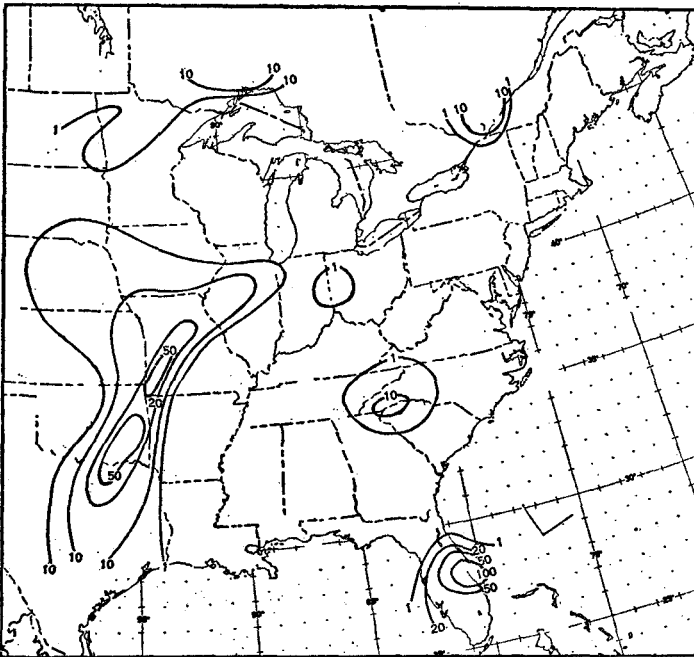


FIGURE 13.—Isohyets of computed precipitation in hundredths of an inch for the 12-hour period 1500 GMT, December 25 to 0300 GMT, December 26, 1949. Compare with figure 14.

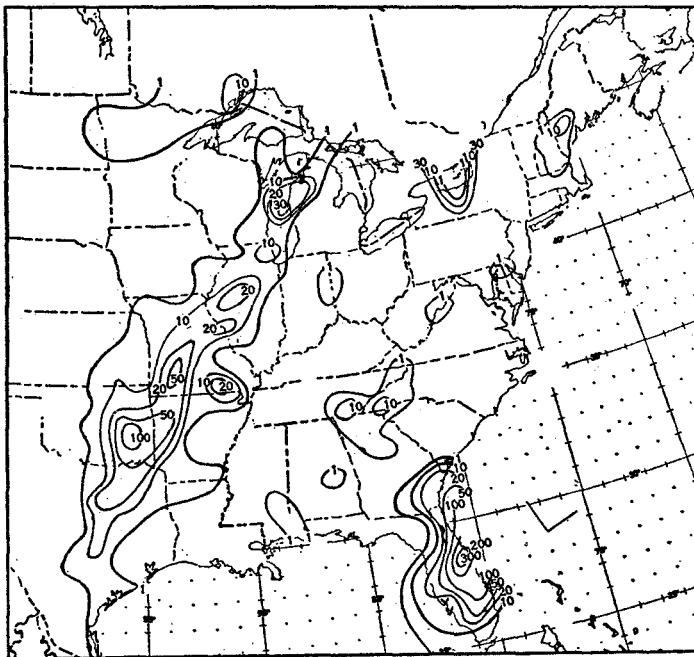


FIGURE 14.—Isohyets of observed precipitation in hundredths of an inch for the 12-hour period 1500 GMT, December 25 to 0300 GMT, December 26, 1949.

important as vertical motion in quantitative precipitation forecasting.

The tendency of the layer from 700 mb. to 500 mb. to over-compute precipitation suggests that cloud storage and evaporation of precipitation falling from high levels may produce large percentage errors when small amounts of precipitation are forecast.

Results also indicate that it will be necessary to consider the effects of topography and skin friction on verti-

cal velocity near the ground. Preliminary studies on these two factors are in progress with encouraging results.

#### ACKNOWLEDGMENTS

Mr. George O. Collins, Short Range Forecast Development Section, and Mr. Jack C. Thompson, Weather Bureau Airport Station, Los Angeles, Calif., advised the author in all phases of this study. Mr. Roger A. Allen, Chief, Short Range Forecast Development Section gave valuable assistance in the final revision of the manuscript. Credit is due Mr. John L. Strong for drafting most of the figures.

Dr. Joseph A. Smagorinsky, Scientific Services Division and Mr. Rodney D. Graham, Weather Bureau Airport Station, Los Angeles, Calif. offered helpful suggestions on the manuscript.

#### REFERENCES

1. J. C. Thompson and G. O. Collins, "A Generalized Study of Precipitation Forecasting, Part 1: Computation of Precipitation from the Fields of Moisture and Wind", *Monthly Weather Review*, vol. 81, No. 4, Apr. 1953, pp. 91-100.
2. J. R. Fulks, "Rate of Precipitation from Adiabatically Ascending Air", *Monthly Weather Review*, vol. 63, No. 10, Oct. 1935, pp. 291-294.
3. G. T. Bennett, "Calculation of the Dilatation of Area from Simultaneous Wind Records at Three Neighboring Stations". Note on p. 102 from *The Life History of Surface Air Currents. A Study of the Surface Trajectories of Moving Air*, W. N. Shaw and R. G. K. Lempfert, Great Britain Meteorological Office (M. O. 174) London, 1906.
4. J. C. Bellamy, "Objective Calculations of Divergence, Vertical Velocity, and Vorticity", *Bulletin American Meteorological Society*, vol. 30, No. 2, Feb. 1949, pp. 45-49.
5. R. D. Graham, "A New Method of Computing Vorticity and Divergence", *Bulletin American Meteorological Society*, vol. 34, No. 2, Feb. 1953, pp. 68-74.
6. R. Fjørtoft, "On a Numerical Method of Integrating the Barotropic Vorticity Equation", *Tellus*, vol. 4, No. 3, Aug. 1952, pp. 179-194.

#### APPENDIX—GRAPHICAL PROCEDURES

##### DIVERGENCE

The steps required for the graphical computation of divergence may be summarized as follows:

1. Analysis of streamlines and isotachs to provide the necessary wind data over the chosen area for the selected levels.

2. Plotting at each vertex of each triangle in the divergence grid (fig. 1), which is printed on a transparent overlay, a wind vector corresponding to 5-hour displace-

ment of the air as indicated by the streamline direction and the isotach field at that point. A 5-hour displacement was chosen because it gave vectors of convenient length for the divergence grid.

3. Reading the partial divergence for each vertex of the triangles along an imaginary line perpendicular to the triangle base opposite each vertex. These imaginary lines are divided, by lines parallel to each of the bases of the triangles, into tenths of each of the altitudes of the triangles. The sample triangle in figure 1 illustrates the partial divergences of .3, -.6, and .2 per 5 hours for each of the vertex vectors readily read off the overlay. It is evident that the geometrical arrangement of the divergence grid in figure 1 effectively cuts the number of partial divergence calculations in half as the absolute values of the partial divergence at any two opposite vertex angles are equal but their signs are opposite.

4. Summing the partial divergence for each triangle, and converting to units of  $10^{-5} \text{ sec}^{-1}$  (fig. 1).

These steps result in a map overlay for each level on which the divergence is plotted at the centroid of each triangle. These overlays are retained for later use. Figure 2 illustrates the streamline-isotach analysis at 950 mb. for 0300 GMT, December 28, 1949, the period used to cover the details of the computations, and figure 1 shows the corresponding plotted divergence overlay.

Several preliminary tests were made to determine the best orientation of the Divergence Grid, for it is fixed by a set of reference coordinates when used over the streamline-isotach charts. In some instances, however, where a narrow, low level "jet" appeared, it was necessary to move the Divergence Grid so that the base line of a group of grid triangles lay along the axis of the "jet". This technique tended to eliminate the extreme non-linearity in the wind field when the core of the "jet" was narrower than the distance between triangles.

#### VERTICAL VELOCITY

As the next step in the computation of a quantitative precipitation pattern, isanabatic charts at the chosen levels are obtained by graphical addition of vertical velocity at the bottom of a layer and divergence within the layer. Equations (5a), (6a), (7) and (8) give the constant multipliers for the various levels, and the following paragraphs give level-by-level procedures.

*Vertical velocity at 950 mb.*—Each of the divergence values on the 950-mb. divergence grid chart is relabeled after multiplication by the factor 0.50, obtained from equation (5a). Working directly from the relabeled divergence grid, the 950-mb. isanabats are analyzed at intervals of one centimeter per second on an acetate overlay, and retained for later use. Figure 3 depicts this field of isanabats, which, together with the 950-mb. divergence analysis is retained for use in the 850-mb. computations.

*Vertical velocity at 850 mb.*—In this step, following equation (6a), graphical addition appears for the first

time. Using the divergence isopleths for 950 mb. previously prepared on acetate, and the analysis of a  $0.50D_{850}$  field on the previously plotted  $D_{850}$  overlay, the two fields are graphically summed. Figure 4 illustrates the technique which results in the isopleths of vertical velocity at 850 mb. illustrated in figure 5.

*Vertical velocity at 700 mb.*—By reference to equation (7), it is apparent that two steps of graphical addition are necessary in the computation of 700-mb. isanabats, since no justifiable approximations could be made in the formula. However, relabeling the  $0.50D_{850}$  isolines by merely doubling their values provides a fair approximation to the  $0.91D_{850}$  isolines. For more precise calculations it would obviously be necessary to analyze  $0.91D_{850}$  isolines. Following the analysis of a  $0.77D_{700}$  chart, the graphical addition of  $-D_{850}$  and  $-0.77D_{700}$  is carried out on acetates. A reanalysis of the  $V_{2850}$  field, as required in equation (7), furnishes the isolines of  $1.17V_{2850}$ . A second graphical addition, involving the sum of  $1.17V_{2850}$  and  $-(D_{850} + .77D_{700})$  then gives the isanabatic field at 700 mb. which is kept for use in the 500-mb. computations. Figure 6 gives the resulting 700-mb. isanabatic field.

*Vertical velocity at 500 mb.*—An inspection of equation (8) indicates that it is necessary to analyze the field of  $1.31V_{700}$  and  $1.28D_{500}$  before performing the two steps of graphical addition that provide the isanabatic field at 500 mb. The  $1.68D_{700}$  field is relabeled by doubling the  $0.77D_{700}$  field and, hence, is an approximation. Performing the required graphical summations provides the field of vertical motion at 500 mb.

*Mean vertical velocity.*—One of the basic assumptions in the original study [1] was that the field of vertical motion remained unchanged throughout the 12-hour period subsequent to the computations. In an attempt to improve upon this assumption, "mean" isanabatic fields may be analyzed by graphically averaging the vertical velocities at the beginning and end of a particular 12-hour period.

#### RATE OF PRECIPITATION

In the moisture computations, the same method is followed for each of the levels for which vertical motion is computed. Consequently it is possible to illustrate this analysis by reference to the 700-mb. level, only, for a typical calculation.

Equation (3) shows that the addition of a moisture term to the vertical motion term gives the effective vertical velocity. The field of  $0.28(T_0 - T_{d0})$  is obtained by plotting the values of this quantity from all available soundings and analyzing the map.  $T_0$  and  $T_{d0}$  are the temperature and dew point at the top of the chosen layers at the beginning of the period. This analysis, together with the entry of the isotherms at  $5^\circ\text{C}$ . intervals required in the evaluation of  $Ik$  is made on acetate over the appropriate upper level charts. Figure 7 illustrates the field of  $0.28(T_0 - T_{d0})$  at 700 mb.

To obtain the effective vertical velocity,  $V'_z$ , isopleths

of  $0.28 (T_0 - T_{a0})$  are subtracted graphically from the isanabatic field for 700 mb. This analysis is carried out on acetate by superimposing the chart represented in figure 7 over the corresponding  $V_z$  chart as shown in figure 6. As computations of precipitation are made only where  $V_z > 0$ , the  $V_z = 0$  isanabat is first traced in color to outline such areas. In these areas, the graphical subtraction is performed to obtain the effective vertical velocity,  $V'_z$ . Colored isopleths are very effective in reducing the possible confusion that may arise due to the many lines appearing on this analysis. Figure 8 illustrates the graphical subtraction required to obtain the  $V'_z$  isopleth field at 700 mb.

The conversion from isopleths of effective vertical velocity to isohyets is made according to equation (9). The term  $Ik$  is evaluated for the areas where  $V_z > 0$  by noting the mean temperature range over those areas and noting the corresponding value of this constant from the values given in table 1. The isolines of  $V'_z$  are multiplied by  $Ik$  and relabeled as isohyets for each of the four levels (See fig. 8).

It is evident from table 1 that the term  $Ik$  is fairly uniform over a wide range of values of  $T_0$ , especially at the lower levels. Thus as this study progressed, it became

clear that this method of evaluating the isohyets produced results closely approximating those values of the isohyets obtained from a logarithmic graphical multiplication of  $Ik$  by  $V'_z$ . The latter method, when required by strong areal variation of  $Ik$ , necessitates graphical addition of the logarithms of the  $V'_z$  field and the logarithms of  $Ik$ . The antilogs of the sum, which are products of the two variables, will give the isohyetal field at each level. However tests indicated, that the logarithmic, graphical technique could give significantly better results only in areas of a large temperature gradient. The analysis of the precipitation contribution from each layer, described above, which assumes no areal variation of  $Ik$ , does not involve any graphical computations, merely necessitating the re-labeling of the  $V'_z$  isolines as isohyets. To obtain the categorical answer, "rain" or "no rain", areas inclosed by the .01-inch isohyet at each level are combined on acetate into a composite precipitation chart for the surface.

The quantitative isohyetal pattern for the surface is made up of the sum of the precipitation contributions from each of the four levels and is readily acquired by four relatively simple, graphical addition steps as indicated by equation (10).